the number of $d^{*+}K^{*-}$ events if one-pion exchange is the dominant production process. We find that $\sigma(K^-d \rightarrow K^{*0}d^{*0})/\sigma(K^-d \rightarrow K^{*-}d^{*+}) = 0.5 \pm 0.4$, which is not inconsistent with 1, especially since the effects of contamination from other final states on this channel are not understood. A better place to investigate the d^*-K^* state would be in the reaction

$$K^-d \rightarrow K^-\pi^+\pi^-d\,, \tag{27}$$

which is a four-constraint fit, and in which only one $K^*(890)$ is allowed.

ACKNOWLEDGMENTS

This experiment was initiated under the leadership of the late Professor George Tautfest. We would like to express our gratitude to the Argonne National Laboratory, in particular, Dr. M. Derrick, Dr. F. Schweingruber, and Dr. L. Voyvodic. We are grateful to Dr. N. Samios and Dr. I. Skillicorn for access to their K^-p data. We wish to express our thanks to our programming group, especially W. Franklin; to our scanning and measuring girls; and to our technical staff.

PHYSICAL REVIEW D VOLUME 2, NUMBER 1 1 JULY 1970

Measurement of the Velocity Dependence of the Helicity of Beta Particles from Co^{60}†

D. M. Lazarus* and J. S. Greenberg

Physics Department, Yale University, New Haven, Connecticut 06520

(Received 13 March 1970)

A series of experiments has been carried out to study the velocity dependence of the helicity $\mathcal{H}$ of β particles from the allowed Gamow-Teller decay in Co^{60}. The energies examined were varied from 205 keV ($v/c = 0.7$) to 50 keV ($v/c = 0.41$), a region where the velocity is changing rapidly with energy, and where several other measurements have reported deviations from $\mathcal{H} = -v/c$. We have not observed any discrepancy with a $-v/c$ dependence for the helicity within a measurement accuracy of a few percent at the highest velocities and 9% at the lowest velocity. The weighted mean of the helicity measurements is $-\mathcal{H}/(v/c) = 1.014 \pm 0.018$. Assuming, in turn, either the two-component neutrino theory with predominantly axial-vector interaction or the absence of any tensor interaction admixture, this result limits the ratio C_T/C_A to < 0.0029, and the ratio C_A'/C_A to values between 0.90 and 1.11. The helicity was analyzed by Mott scattering after transformation of the polarization from longitudinal to transverse. A screened Mott scattering function $S(\theta)$ was used in the analysis. The behavior of depolarization effects and the other systematic errors associated with the technique as a function of β-particle energy was investigated extensively, and the influence of these effects on the results is reported.

I. INTRODUCTION

The $V-\lambda A$ form for the four-fermion interaction provides a consistent representation for the extensive experimental information now available on the strangeness-conserving weak decays.[1–7] At low energy, investigations in nuclear β decay of spectral shapes, ft values, β-ν correlations, the β asymmetry from polarized nuclei, β-γ (circular polarization) correlations' the helicity of the neutrino, and the helicity of β particles have furnished some of the definitive tests for the $V-\lambda A$ theory with conserved vector current and maximum parity violation, and have determined a number of its important parameters. We may note, however, that there is considerable experimental uncertainty associated with the measurements of some of these parameters which allows for significant departures from the predictions of the theory. These uncertainties reflect, in part, the difficulties of the measurements, and in some cases the poor sensitivity with which the β-decay parameters can be extracted from the measured quantities noted above.

The latter situation, for example, occurs in the determination of the relative magnitudes of the parity-conserving and the parity-nonconserving coupling constants, C'/C. It is a characteristic feature of the experiments from which this ratio may be deduced that the functional dependence of the measured pseudoscalar quantities on the ratio C'/C always occurs in the form

$$\frac{C'/C}{1+(C'/C)^2}\,,$$

† Research (Yale Report No. 2726-561) supported by the U. S. Atomic Energy Commission under Contract No. AT(30-1)2726, and the National Science Foundation.

* Present address: Brookhaven National Laboratory, Upton, N. Y.

1 T. D. Lee and C. S. Wu, Ann. Rev. Nucl. Sci. **15**, 381 (1965).

2 C. S. Wu, Rev. Mod. Phys. **31**, 783 (1959); **36**, 618 (1964).

3 M. Deutsch and O. Kofoed-Hansen, in *Expermiental Nuclear Physics*, edited by E. Segrè (Wiley, New York, 1959), Vol. 3.

4 E. J. Konopinski, Ann. Rev. Nucl. Sci. **9**, 99 (1959).

5 R. J. Blin-Stoyle, in Proceedings of the Topical Conference on Weak Interactions, CERN, 1969, p. 497 (unpublished).

6 *Alpha-, Beta-, and Gamma-Ray Spectroscopy*, edited by Kai Seigbahn (North-Holland, Amsterdam, 1965), Vol. 2, Chaps. XXIII–XXIV.

7 References 1–6 are review articles. References to original work are given there.

so that near-maximum-parity-violation high-precision experiments are required to set even modest limits on the possible deviation of C'/C from the value of unity. The more precise determinations of this ratio for Gamow-Teller transitions derive from measurements of the helicity of β particles and β-γ (circular polarization) correlations.[6] In these cases, the uncertainty in evaluating C'/C from data encompassing a substantial range of β-particle velocities exceeds 25%. For Fermi transitions the poor accuracy of the available helicity measurements allows considerably larger departures of C'/C from unity.[6] We also note here that for β-particle energies below a few hundred keV, the experimental situation is even less favorable, with large systematic uncertainties severely limiting the accuracy with which the expected velocity dependence for the helicity and the β-γ (circular polarization) correlation can be verified. Examination of measurements of other parameters of the theory indicates that accurate determination of a number of β-decay parameters is desirable.

Precision measurements of the helicity of β particles emitted from unpolarized nuclei provide one method of further extending the experimental accuracy with which some of the β-decay parameters have been determined. Neglecting the small corrections arising from finite nuclear size, higher-order transitions, and interactions with atomic electrons, the $V-\lambda A$ theory with two-component neutrinos ($C'=C$) predicts that the helicity of electrons emitted in allowed β decay is $-v/c$. This velocity dependence has been confirmed for v/c greater than 0.7 by a number of experimental techniques and for a variety of β emitters with uncertainties between a few percent and 20%.[6] In the interesting region below $v/c=0.7$, where the velocity varies rapidly with energy, the measurements have been subject to large uncertainties and the experimental behavior of the helicity with energy has remained ambiguous, with several low values reported.[8–10] These low values have been attributed in part to a variety of depolarization processes usually evaluated with large uncertainties; however, in some experiments deviations from a helicity of $-v/c$ remain after all known corrections have been applied.[9,10] It is clear that precise measurements become increasingly difficult as the energy decreases, because of the multiplying uncertainties in evaluating systematic errors at the lower β energies. Reflecting these difficulties, the momentum dependence of the helicity has not been investigated in sufficient detail for a single transition at the lower momenta to permit a meaningful comparison with theory.

Herein we report on a series of measurements on the velocity dependence of the helicity of β particles emitted in the decay of Co^{60} with velocities ranging between $0.41c$ and $0.70c$. Quoted for 1-standard-deviation uncertainties, these measurements set upper limits of 0.10 and 0.0029, respectively, for $|1-C_A'/C_A|$ and for the ratio of tensor to axial-vector coupling coefficients C_T/C_A. A preliminary report on this work was presented at the International Conference on Weak Interactions in 1965.[11] Concurrent and related measurements, reporting the low helicities referred to above, have been performed at other laboratories.[9,10] We have completed additional measurements since the 1965 report, including more comprehensive investigations of the influence of systematic errors upon the results. This paper summarizes these studies as well as measurements performed at an earlier time but not previously reported in detail.[12]

II. EXPERIMENTAL METHOD

The Mott scattering method for helicity analysis used in the previous measurement[13] in this laboratory was again employed for these investigations. Of the known electron helicity analyzers, it potentially is the best method available for helicity measurements for the lower velocity region ($v/c<0.7$) on which these measurements focus. Although the apparatus has been considerably altered to provide increased transmission, greatly improved detector energy resolution, and a reduction in sensitivity to γ-ray background and electrons scattered from the walls, the reader is referred to the earlier work[13] for many of the details of the experimental method and a comprehensive listing of references to the relevant literature up until 1960.

The Mott scattering analysis of electron helicity utilizes the spin-dependent asymmetry in the scattering of electrons by the Coulomb field of an atomic nucleus. The cross section is

$$\frac{d\sigma}{d\Omega}(\theta,\varphi)=\left[\frac{d\sigma}{d\Omega}(\theta)\right]_0[1-P_TS(\theta)\sin\varphi], \tag{1}$$

where $[d\sigma/d\Omega(\theta)]_0$ is the spin-independent differential cross section, $S(\theta)$ is the asymmetry function which has been calculated by Sherman[14] for scattering by a point nucleus, and more recently by Lin,[15] Holzwarth and Meister,[16] and Bühring,[17] who include screening by

[8] M. Bienlein, K. Güthner, H. Von Issendorff, and H. Wegener, Nucl. Instr. Methods **4**, 79 (1959); Z. Physik **154**, 376 (1959).

[9] V. Eckardt, A. Ladage, and U. V. Moellendorff, Phys. Letters **13**, 53 (1964).

[10] J. Van Klinken, Nucl. Phys. **75**, 145 (1966).

[11] J. S. Greenberg and D. M. Lazarus, in Proceedings of the Argonne International Conference on Weak Interactions, 1965 (ANL Report No. ANL-7130), p. 313 (unpublished).

[12] D. M. Lazarus and J. S. Greenberg, Bull. Am. Phys. Soc. **9**, 28 (1964); **10**, 424 (1965); D. M. Lazarus, Ph.D. dissertation, Yale University, 1965 (unpublished).

[13] J. S. Greenberg, D. P. Malone, R. L. Gluckstern, and V. W. Hughes, Phys. Rev. **120**, 1393 (1960).

[14] N. Sherman, Phys. Rev. **103**, 1601 (1956).

[15] S. R. Lin, Phys. Rev. **133**, A965 (1964).

[16] G. Holzwarth and H. J. Meister, Nucl. Phys. **59**, 56 (1964); *Tables of Asymmetry, Cross Section and Related Functions for Mott Scattering of Electrons by Screened Gold and Mercury Nuclei* (Institut für Theoretische Physik der Universität München, Germany, 1964).

[17] W. Bühring, Z. Physik **212**, 61 (1968).

atomic electrons. The maximum asymmetry in the single scattering of an electron of transverse polarization P_T through an angle θ occurs at $\varphi=\pm\pi/2$ in azimuth relative to the plane of the initial momentum and polarization vectors. The asymmetry is then defined in terms of the left and right scattered intensities L and R by

$$A\equiv\frac{L-R}{L+R}=\frac{d\sigma/d\Omega\,(\theta,+\pi/2)-d\sigma/d\Omega\,(\theta,-\pi/2)}{d\sigma/d\Omega\,(\theta,+\pi/2)+d\sigma/d\Omega\,(\theta,-\pi/2)}=-P_T S(\theta)\,. \quad (2)$$

As has been emphasized in the past,[13] interpretation of Eq. (2) in terms of the experimentally observed scattering asymmetry requires consideration of various corrections which modify the measured asymmetry. These derive principally from spurious instrumental asymmetries not associated with spin-dependent scattering, multiple and plural scattering in the scatterer, source and source-backing depolarization, and depolarization effects due to scattering in the apparatus. The increasing influence of these effects as the energy of the β particle decreases has impeded the extension of helicity measurements to lower energies. Further difficulties are encountered at the lower energies because of β-particle detection problems arising from resolution limitation of available detectors and enhanced sensitivity to the background.

In order to extend the new helicity measurements to lower energies, a number of changes were made in the apparatus reported earlier.[13] The most important of these are a tenfold increase in the transmission of the apparatus, greater resolution and better discrimination against background through the use of cooled surface-barrier detectors and low-noise electronics, improved collimation of the electron beam, and, most important, the utilization of thinner scattering foils and sources which was made possible by the other modifications.

A. Apparatus

The experimental arrangement is shown schematically in Fig. 1. The electrostatic analyzer, which provides energy selection and conversion of the polarization from longitudinal to transverse, is preceded by a magnetic quadrupole doublet. The lack of vertical focusing (perpendicular to the plane of the figure) by the electrostatic field is compensated by the astigmatic quadrupole lens to produce approximately a factor of 10 increase in transmission over that attainable with the cylindrical electrostatic lens alone. The magnetic field gradients were chosen so that the component of the beam divergent from the source in the plane of electrostatic

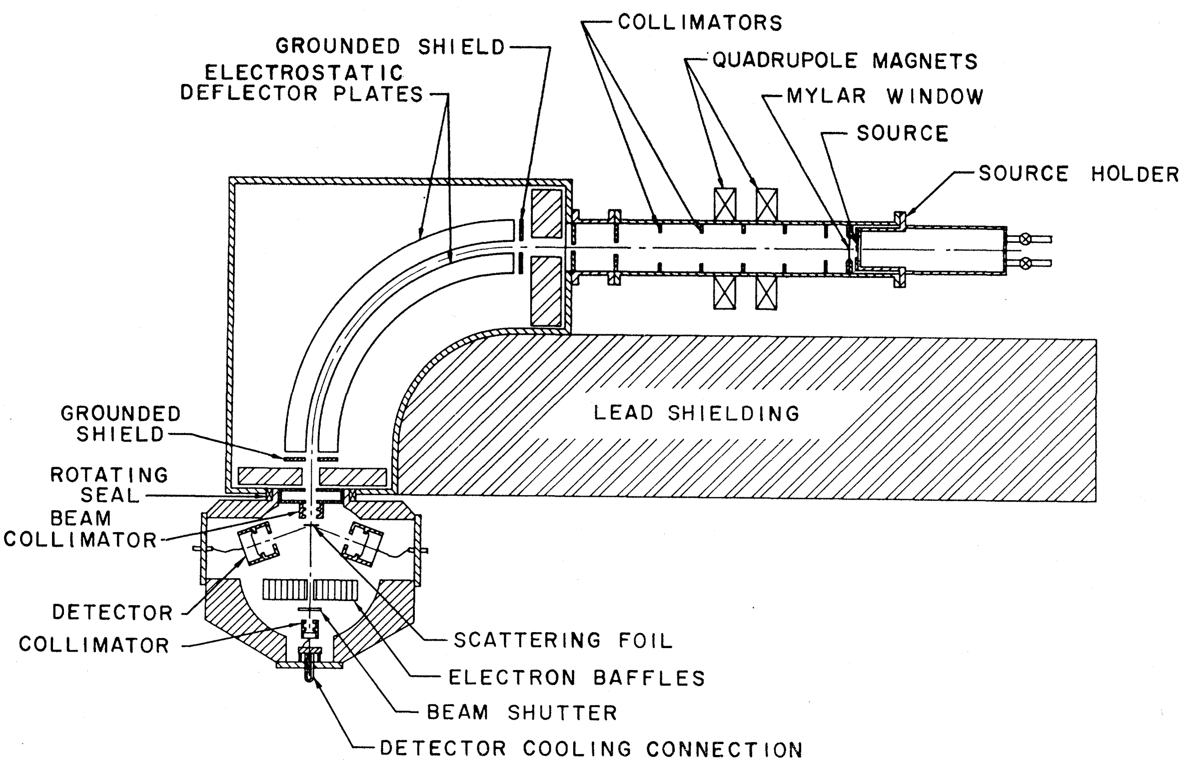

FIG. 1. Schematic plan view of the Mott scattering apparatus showing the magnetic quadrupole lenses, the 90° electrostatic analyzer, and the scattering chamber. The detectors are shown in the position where the asymmetry is a minimum. The individual components have been drawn in a simplified version for clarity of presentation.

deflection (the horizontal plane) was focused at the object position for the electrostatic lens, whereas the vertical component converged at the image plane, i.e., at the scattering foil, after passing through the deflecting field. In operating the magnetic lens astigmatically, the maximum angular divergence in the horizontal plane at the analyzer input is matched to the maximum acceptance angle for the analyzer so that no loss of intensity is incurred in the horizontal plane while the additional focusing in the vertical plane increases the over-all transmission of the system. The magnetic lens and the collimators in the vacuum pipe preceding the electric field region also provide a preselection of the energy (20%) before the beam enters the electrostatic analyzer, which reduces the contributions to the beam from electrons which can reenter the beam after scattering from the high-voltage plates. The transmission of the system is $\sim 5\times 10^{-4}$, with an energy resolution of 5%.

The electrostatic analyzer has been discussed in detail in the earlier paper.[13] The high voltage was monitored with an accuracy of one part in 10^5 by a potentiometer measuring the voltage across the last resistor in a high-voltage chain which was immersed in an oil bath. The equality of the positive and negative supplies was established with a similar degree of precision by measuring their voltage sum with respect to ground with a vacuum tube voltmeter. The energy calibration of the analyzer and magnetic lens was carried out with sources of internal conversion electrons, and the correlations between the settings for the magnetic lens and electrostatic analyzer that produced maximum transmission were carefully studied.

The scattering chamber was constructed with a rotary seal so that the azimuthal angle of scattering was varied by rotating the whole chamber. Thus the relative positions of the counters and scattering foil remained constant as the azimuthal angle was varied, which ensured that the solid angle subtended by the scattering foil at the counters also remained constant as a function of the azimuthal angle selected. This arrangement minimized spurious asymmetries that arise from nonuniformities in the scattering foil. The three detectors and five scattering foils were positioned with precision jigs constructed for this purpose, and the system alignment and symmetry with respect to the scattering chamber axis were verified by cathetometer measurements. The orientations of the planes of the scattering foils were adjusted perpendicular to the axis of rotation of the scattering chamber by using the scatterer as a mirror in an optical lever arrangement. Particular precaution was taken with the absorption of the primary beam by baffles after passing through the scatterer to prevent secondary scattering into the counters. Measurements indicated that background contributions from wall scattering, either from secondary scatterings after initial scattering by the scattering foil or scatterings of the primary beam, were a small part of the total background rate.

The scattered electrons were detected with two liquid-nitrogen-cooled 450-mm^2 silicon surface-barrier detectors positioned at a polar angle of 70° to the incoming beam and 180° apart in azimuth. Each counter subtended an angle of $\pm 10°$ measured from the foil center. Two detectors were employed to both increase the data accumulation rate by a factor of 2 and reduce the sensitivity of the measurement to spurious asymmetries that may arise from instabilities of the apparatus, such as the time variation of the beam intensity. Such instabilities reflect in both counters equally and their effect on the asymmetry is eliminated when ratios such as Eq. (3) are formed. In addition to these two detectors, a third detector, preceded by a small collimator, monitored the stability of the beam. The silicon surface-barrier detectors that were employed provided the needed resolution and the low sensitivity to γ radiation which is required to extend the helicity measurements to energies as low as 50 keV without preacceleration before scattering. Without preacceleration, this low-energy region has not been readily accessible to measurement with scintillation-counter techniques. We note that although the use of preacceleration has the advantage of confining the scattering to a single energy, independent of the initial β-particle energy, new sources of systematic error are introduced by its use which are associated with the accelerator optics and stability. A scattered-electron spectrum is shown in Fig. 2. The full width at half-maximum for the scattered spectra was typically less than 13 keV, with a significant contribution coming from the finite spread in the electron beam energy. This improved resolution not only contributed to the general

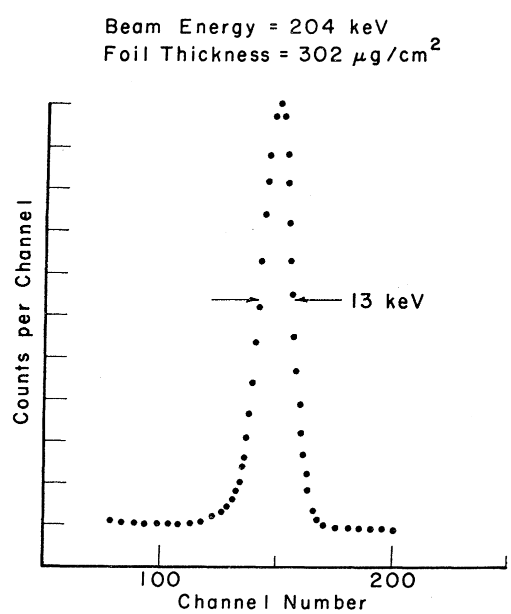

FIG. 2. Counter spectrum of 200-keV electron scattered from a gold foil. The full width at half-maximum is 13 keV, of which 10 keV is contributed by the beam energy spread.

quality of the data by greatly enhancing the rate of data accumulation due to improved signal–to–γ-ray background, but it also facilitated the investigation of the effect of secondary scattering from the walls and collimators of the apparatus on the measured asymmetry.

As in our previous measurements,[13] a forward scattering angle of 70° was chosen principally as a concession to intensity considerations and the desire to stay in the transmission direction to minimize multiple and plural scattering effects in the scattering foil while utilizing two counters separated 180° in azimuth. The latter consideration becomes particularly significant at the lowest energies investigated, since, as has already been emphasized, the multiple and plural scattering effects become increasingly important in the polarization analysis at the low energies and contribute largely to the uncertainty in the measurement, even for thin scattering foils. In general, the ratio of multiple and plural scattering to single scattering is smaller in the forward direction than for backward scattering. It has also been shown[13,18] that the contribution of electrons detected after having been initially scattered into the plane of the foil is particularly difficult to estimate theoretically, and since their distribution should be nearly symmetric about the plane of the foil, they will be proportionally reduced in the forward-scattered intensity because of the larger cross section for single scattering. Another important advantage of operating at forward scattering angles is the greater facility with which the counters can be shielded from electrons which scatter from the scattering chamber walls and dilute the measured asymmetry. However, the scattering geometry chosen necessarily yields smaller scattering asymmetries than are available at the more backward angles. In connection with the choice of scattering angle, it is also interesting to note that the Mott scattering measurements for β particles with $v/c<0.6$ have been performed with backward scattering geometries and have yielded magnitudes of the helicities $<v/c$.[8–10]

Gold scattering foils were used since the large atomic number yields a large asymmetry in the spin-dependent scattering, and foils with a uniform surface density can be prepared by vacuum evaporation onto extremely thin Formvar backings. The error in the extrapolation procedures by which the asymmetry in Eq. (2) is extracted from the measured asymmetry with foils of finite thickness depends in part on the uncertainty in the determination of the foil thickness. Three methods were therefore used to obtain relative and absolute surface densities and to examine the nonuniformities.

(1) The absolute average thickness was determined by weighing with a microbalance to a nominal accuracy of $\pm 5\,\mu$g. This provided the absolute calibration required for the other two measurements.

(2) The range attenuation technique with a collimated beam of α particles[19] was used to examine the macroscopic uniformity of the foil surface and the relative thickness of the foils. Repeated measurements covering the scatterer surface showed only statistical fluctuations indicating macroscopic uniformity of better than 1%.

(3) The relative thickness of the foils was also measured with small-angle scattering of 600-keV electrons. A scattering chamber was connected to the output of a β-ray spectrometer and the scattered intensities were measured at 40°. This method provided the most accurate relative values of the scatterer thickness since plural and multiple scattering are negligible at this energy and angle.

The scatterers used covered a range from 41 to 302 μg/cm^2 on Formvar backings of 15–20 μg/cm^2, and these surface densities were determined to an accuracy of $\pm 2\,\mu$g/cm^2. The three methods yielded values of the relative thickness which were consistent within the errors quoted.

The rapid variation of the asymmetry function and of the differential scattering cross section with scattering angle necessitates an integration of the product $S(\theta)d\sigma/d\Omega\,(\theta)$ over the scatterer and detector areas. The detector areas were precisely determined by collimators. In order to specify the scattering area independent of the beam dimensions and small fluctuations in position, the scattering foils were prepared by evaporation through a circular aperture placed directly in front of the Formvar backing which precisely determined the area covered by the gold. The gold area was considerably smaller than the electron beam cross section, which in turn was smaller than the circular Formvar cross section. The electron beam uniformity over the scatterer area was checked with x-ray film exposures. Optical densitometer traces indicated that the nonuniformities in the beam were less than a few percent.

Depolarization effects in the source and its backing were studied by varying both the source and backing thicknesses. Particular attention was devoted to these studies because of the unduly large depolarizations attributed to scattering within the source that have been reported in the literature.[9] Sources of 25 and 12 mCi with surface densities of 345 and 170 μg/cm^2 were uniformly electroplated on nickel backings of 0.9 mg/cm^2. Additional backings were introduced during the course of the experiment as will be described below. The source mount was constructed with a large evacuated volume behind the source. The walls of the vacuum chamber were lined with low-atomic-number material and electron baffles to minimize scattering from the holder. The source assembly was separated from the main volume by a 0.00025-in. aluminized Mylar window and was maintained under vacuum independently.

[18] R. L. Gluckstern and S. R. Lin (private communication).

[19] W. C. Barber, Rev. Sci. Instr. 24, 469 (1953).

The data accumulation procedure consisted of accumulating scattered-electron spectra for both detectors at one scattering chamber orientation corresponding to an azimuthal scattering angle φ for one counter. The scattering chamber was then rotated 180°, thereby interchanging the detectors, and the measurement was repeated for an equal time interval. This procedure eliminated to first order spurious asymmetries which derive from differences in detector sensitivity, resolution, and alignment. The number of events within the full width at half-maximum as well as larger cuts of the scattered spectra were used in the analysis procedures in order to check the effect of the various background contributions on the asymmetry. The results from these comparisons are discussed below.

The data on the scatterer-thickness dependence of the asymmetry were accumulated for time intervals which gave equal counting statistics for each scatterer except the thickest. The maximum counting interval was 1 h; the thickest scattering foil, as well as the thinnest, was run for this period in order to obtain greater statistical accuracy in the measurement of the source-backing-thickness dependence, in which only the thickest foil was used. Background and the contribution of electrons scattered directly into the detectors by the Formvar backings were evaluated by periodically taking data with a Formvar backing on which gold had not been evaporated. The Formvar backing contributed 10% of the counting rate for the 41-μg/cm^2 gold scatterer and approximately 1% for the 302-μg/cm^2 foil within the full width at half-maximum of the scattered spectra. Inspection of the total scattered spectrum indicated that more than 70% of the background spectrum was contributed by the Formvar, with the remainder due largely to γ rays. This is consistent with the background rates obtained with sources in which γ-ray transitions were absent. Electronic drifts were monitored and compensated continuously.

B. Evaluation of Systematic Errors

1. *Geometric Asymmetry*

The influence of instrumental asymmetry and depolarizing effects was evaluated following the analysis reported in the earlier paper.[13] The asymmetry A can be written in terms of the scattered intensities $I_1(\varphi)$, $I_1(\varphi+\pi)$, $I_2(\varphi)$, and $I_2(\varphi+\pi)$ as

$$A=\frac{[I_1(\varphi)I_2(\varphi)/I_1(\varphi+\pi)I_2(\varphi+\pi)]^{1/2}-1}{[I_1(\varphi)I_2(\varphi)/I_1(\varphi+\pi)I_2(\varphi+\pi)]^{1/2}+1}=\frac{L/R-1}{L/R+1}, \tag{3}$$

where I_1 and I_2 refer to the counting rates in detectors 1 and 2, respectively, and φ refers to an azimuthal angle measured relative to φ_0, the plane defined by the momentum and polarization vectors. The ratio L/R in Eq. (3) is thus obtained from the geometric mean of the left and right scattered intensities as measured in the two orientations of the scattering chamber. Because the spin-dependent asymmetry decreases with decreasing energy, the spin-independent instrumental asymmetries increase in relative importance, since they remain relatively constant in magnitude.

It has already been pointed out that all asymmetries arising from lack of precision in relative positioning of detectors and scatterers vanish as a consequence of the fixed relative positions of the scatterer and counters as the scattering chamber is rotated. Similarly, spurious effects which arise from rotation of the scattering chamber and which reflect in the two counters in an identical fashion, such as the variation in the average energy of the beam due to any lateral movement of the scattering chamber axis relative to the beam axis as the azimuth is varied, do not produce any measurable asymmetry as it is defined in Eq. (3). Studies of the asymmetries that can be generated by beam nonuniformities indicate that the measured degree of uniformities in the beam and scatterers ensures that asymmetries arising from this source are negligible. The dominant source of geometric asymmetry is the angular misalignment of the beam axis and the axis of rotation of the scattering chamber.

In the previously reported analysis it was shown that an angular misalignment θ', φ' between the beam axis and the rotation axis of the scattering chamber leads to an asymmetry of the form

$$A\approx\left(\theta'\frac{|\partial\eta/\partial\theta|}{\eta}\sin\varphi'-P_TS(\theta)\cos\varphi_0\right)\sin\varphi+\left(\theta'\frac{|\partial\eta/\partial\theta|}{\eta}\cos\varphi'+P_TS(\theta)\sin\varphi_0\right)\cos\varphi, \tag{4}$$

where

$$\eta=\left[\frac{d\sigma}{d\Omega}(\theta)\right]_0.$$

The angle θ' between the beam axis and the rotation axis of the detectors is principally the result of two effects: the deflection of electrons in the magnetic field of the earth and the adjustment of the magnetic quadrupole optics. The horizontal component of the earth's field in the laboratory is 0.18 G, which can produce values of θ' between 9 and 20 min of arc, leading to geometric asymmetries of 0.008 to 0.016 for our measurements. This spread arises from the dependence of θ' upon energy since $|\partial\eta/\partial\theta|/\eta$ is essentially constant for this energy range. θ' was reduced by canceling the magnetic field and by deliberately misaligning the source and quadrupole doublet. It was found that by tuning the system for maximum transmission with the source and magnet positions as variables (these could be changed by means of a micrometer screw and jacks, respectively), the geometric asymmetry was reduced to values ranging between 0.0005 and 0.0040.

These geometric asymmetries were measured using the unpolarized conversion electrons emitted by Cd^{109} and In^{114m}. Sources containing the two emitters electroplated together as well as separately were employed. The measurements were corrected for the polarized electrons produced in the β decay of the In^{114} ground state. The corrections were estimated by integrating the normalized β spectrum over the energy band transmitted by the system. The In^{114} β-particle helicity was taken to be $-v/c$. (The spectrum shape and polarization for first-forbidden Coulomb transitions are predicted by theory and verified by experiment[6,10] to be similar to the allowed decays.) For the composite sources, the In^{114} contributed 5–20% of the electrons transmitted when the system was set on the Cd^{109} conversion lines. The corrected asymmetry was consistent with measurements made with a pure Cd^{109} source.

The assumption that the conversion electrons are unpolarized was verified by searching for a scatterer-thickness dependence of the Mott scattering asymmetry. Comparison of the asymmetry obtained with foils of 41 and 302 $\mu g/cm^2$ for the 84-keV conversion line in Cd^{109} set an upper limit of 2% on the polarization of internal conversion electrons from Cd^{109}.

The results of a measurement on the 163-keV K-conversion line in In^{114m} are shown in Fig. 3, which also illustrates the difference between the asymmetries obtained when all the scattered electrons are detected and when only the full width at half-maximum of the elastic peak is used in the analysis. The small differences at $\varphi=90°$ in the two asymmetries is due to electrons that have undergone secondary collisions in the apparatus. The energy dependence of the geometric asymmetry decreased slightly with energy for the particular compensations made for canceling the earth's field.

2. Plural and Multiple Scattering Effects

It has already been emphasized that a major uncertainty in the Mott scattering analysis of polarization has been the depolarizing effect of plural and multiple scattering, and that this effect is particularly important in the region below 120 keV. In the case of scattering from a foil of small but finite thickness, the scattered intensity may be expanded in powers of scatterer thickness. Keeping terms up to second order in the scatterer thickness t the scattered intensity for polarized electrons can be written in the form[13]

$$dn \approx Nt\left[\frac{d\sigma}{d\Omega}(\theta)\right]_0 \times\{(1+at)[1+P_T S(\theta)\sin\varphi]-btP_T S(\theta)\sin\varphi\}. \quad (5)$$

Similarly, expanding the inverse of the asymmetry in t, and retaining only terms consistent with the second-order terms kept in Eq. (5), yields

$$1/A \approx (1+bt)/P_T S(\theta). \quad (6)$$

In Eq. (6) it was assumed that at and bt are small compared to unity, a limitation which is no more serious than the neglect of higher terms in Eq. (5). The range of validity of Eq. (6) and of extrapolating $1/A$ to zero scatterer thickness has been discussed in our earlier publication,[13] and further investigated in this work.

Gluckstern and Lin[18] have calculated the polarization-independent part of the scattered intensity for several angles and energies. The results are in good agreement

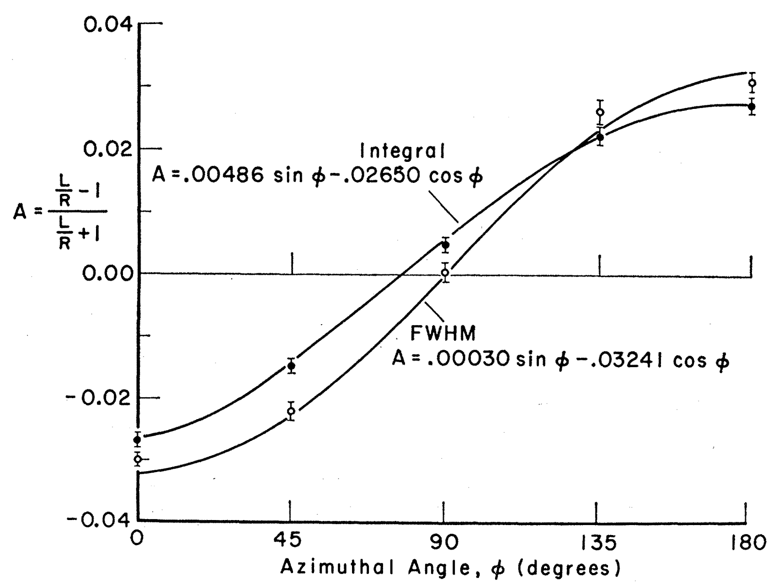

FIG. 3. Azimuthal dependence of the geometric asymmetry that was obtained for the 163-keV conversion electrons from In^{114m}. The solid lines are least-squares fits to the data. The "Integral" curve refers to all scattered electrons detected, while "FWHM" refers to the electrons contained in the full width at half-maximum of the elastically scattered peak.

$$L/R=\left[\frac{I_1(\varphi)}{I_1(\varphi+\pi)}\times\frac{I_2(\varphi)}{I_2(\varphi+\pi)}\right]^{1/2},$$

where I_1 and I_2 refer to counting rates in counters 1 and 2 at the specified azimuthal scattering angle φ which is measured relative to the plane defined by the momentum and polarization vectors.

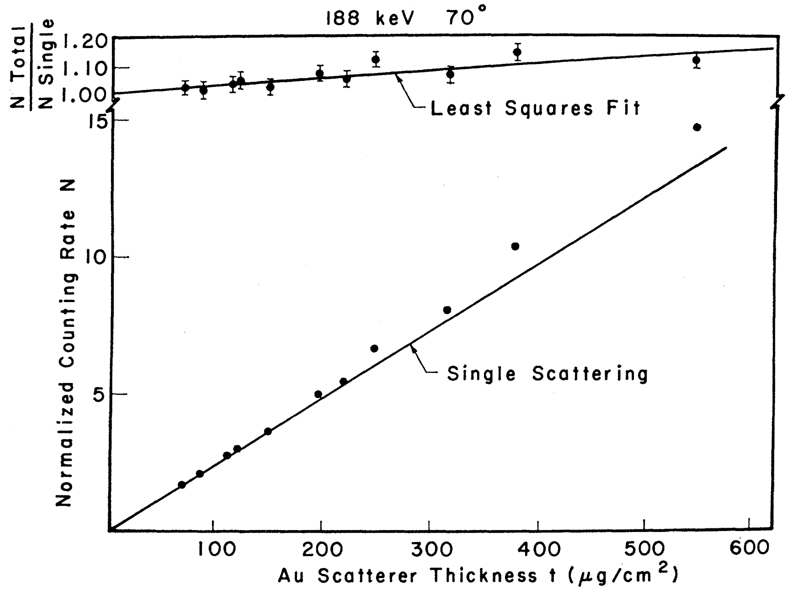

(a)

FIG. 4. Multiple scattering data for (a) 188 keV at 70°, (b) 120 keV at 70°, (c) 188 keV at 110°. The upper graph in each case represents the counting rate divided by the scatterer thickness versus the scatterer thickness with the least-squares fit normalized to unity intercept so that the slope is the coefficient a, the polarization-independent component of the multiple scattering. The lower graph gives the counting rate versus scatterer thickness with the single-scattering contribution plotted as a straight line.

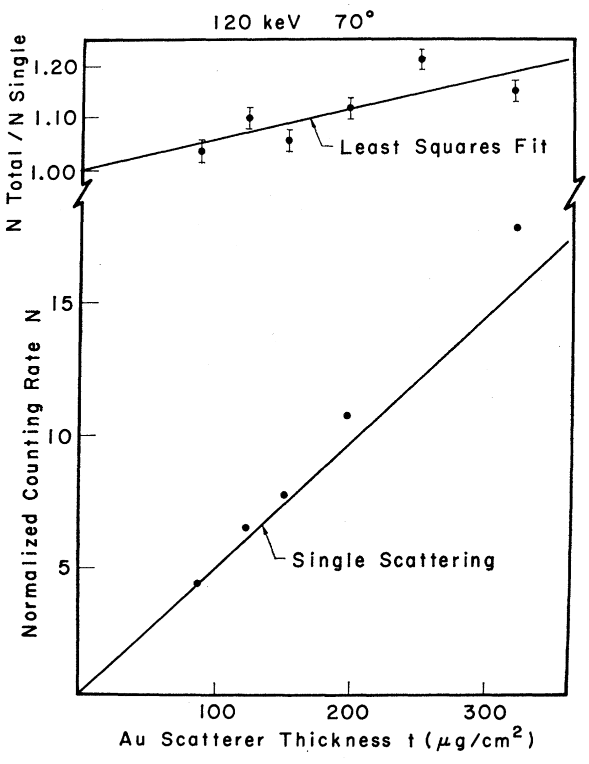

(b)

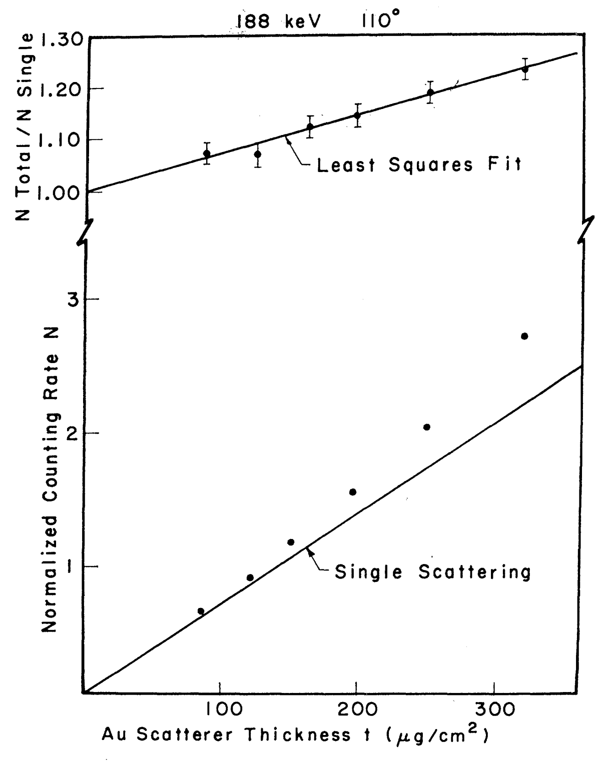

(c)

with those obtained by Wegener[20] from multiple scattering theory and subsequently corrected for numerical errors and modified by Gluckstern.[13] The possible contribution of a $t^2 \ln t$ term arising from in-plane scattering in Wegener's multiple scattering approach has been investigated by Gluckstern. The calculations indicate the $\ln t$ term to be smaller than estimated by Wegener. Numerical calculations of $1/A$ as a function of t have also been carried out by Gluckstern and Lin.[18]

To verify these calculations an experiment was performed in which the polarization-independent part

[20] H. Wegener, Z. Physik **151**, 252 (1958).

of the scattered intensity appearing in Eq. (5) was measured at 70° and 110° at 188 keV and 70° at 120 keV to determine a at these energies and scattering angles. Additional data were obtained at energies of 50, 79, 128, and 204 keV at a scattering angle of 70° during the asymmetry measurements. These are consistent with the data at 128 and 188 keV, although they are less precise. This loss in precision reflects our inability to monitor the beam normalization continuously during the asymmetry measurements. Accurate beam normalization was relatively unimportant for the asymmetry measurements. Particular attention was paid to beam monitoring during the multiple scattering studies. The scattering chamber employed for the multiple scattering experiments differed from the one illustrated in Fig. 1 in that it was larger in order to reduce wall scattering when backward scattering angles were investigated, and it readily allowed the scattering angle to be varied.

Some of the data obtained in the multiple scattering studies are presented in Fig. 4. The lower plot in each case gives the counting rate as a function of scatterer thickness, while the upper graph represents the counting rate divided by scatterer thickness as a function of scatterer thickness. Linear fits to the upper set of data points were normalized so that the intercepts were unity (no multiple or plural scattering at zero scatterer thickness) and the slopes can be directly expressed in percent multiple and plural scattering. The single-scattering contribution obtained from the normalization is indicated in the lower graphs so that the quadratic dependence of the scattered intensities on t is apparent. The resulting multiple scattering contributions to the scattered intensity are compared with the calculated values[18] in Table I(A). The experimental values of the coefficient a are one-third to one-half the calculated values.

The variation of the inverse of the asymmetry with scatterer thickness for the Co^{60} polarization measurements is given in Fig. 5. The data are corrected for geometric asymmetry. It is clear that multiple and plural scattering are quite important at the lower energies. For the measurements at $v/c=0.41$, the reduction in asymmetry is 42% per 100 $\mu g/cm^2$. Weighted least-squares fits were made to the data using quadratic functions as well as the linear ones shown. No statistically significant quadratic effect appeared, i.e., the fits exhibited variations in sign of the coefficient of the quadratic terms. These terms were small enough to produce a negligible effect on the extrapolations. The calculated[18] and measured values of the coefficients a and b are summarized in Table I. No satisfactory explanation for the discrepancies between the experimental and calculated values has been developed, but the data do indicate that the linear extrapolation of the inverse of the asymmetry to zero scatterer thickness is justified for the experimental conditions employed and the accuracy presently obtained.

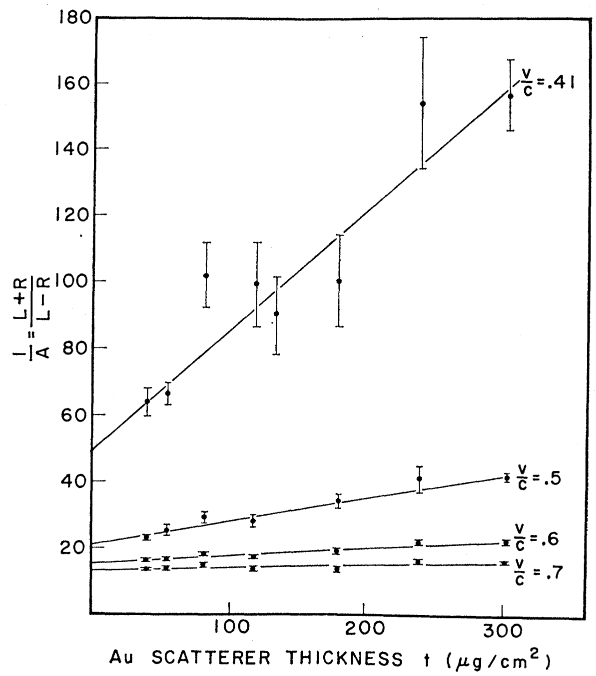

FIG. 5. Inverse of the measured asymmetry versus Au scatterer thickness for Co^{60} β particles with $v/c=0.70$, 0.60, 0.50, and 0.41. The solid lines are least-squares linear fits to the data. The source was electroplated on a 0.9-mg/cm² Ni backing.

TABLE I. (A) Comparison of measured multiple scattering contributions with calculations by Gluckstern and Lin. (B) Comparison of measured reductions in asymmetry due to multiple scattering with calculations by Gluckstern and Lin.

		(A)	
Energy (keV)	Scattering angle (deg)	Multiple scattering per 100 $\mu g/cm^2$ (%) Lin calculation[a]	Experiment
188	70	8.5	2.49±0.24
120	70	13.5	6.12±2.69
188	110	22.0	7.31±0.63
		(B)	
Energy (keV)	Scattering angle (deg)	Reduction in asymmetry per 100 $\mu g/cm^2$ (%) Lin calculation[a]	Experiment
205	70	6	9.3 ±1.6
128	70	16	15.2±1.5
79	70	20	25.2±1.6
50	70	32	42.9±4.2

[a] S. R. Lin (private communication).

3. Backscattering from Source Backing

The depolarization of the electron beam by electrons backscattered from the source backing is another major source of systematic error. As in the case of multiple scattering in the scattering foils, this is a problem that becomes increasingly important with decreasing energy. Electrons scattered at 180° in a single scattering tend to retain their spin orientation in space. If they contribute to the electron beam following such a scattering, they would reduce the beam polarization because of their reversed helicity. However, in general the magnitude of the depolarization is very difficult to estimate since the multiple scattering arguments presented in the case of the scattering foils apply with the added complication that the variation of the spin orientation in the scattering must be accounted for. In the absence of detailed theoretical estimates, the corrections for backscattering from the source backing were made empirically.

Additional backings of 0.9, 2.25, and 4.5 mg/cm^2 (providing total backings 2, 3.5, and 6 times the original thickness) were inserted behind the foil on which the source was electroplated. The asymmetry was then measured with each of these backings in position with the 302-μg/cm^2 scatterer at all four energies. In order to test for effects that may arise from a possible small separation (<0.001 in.) between the source and the added backings, the measurements were repeated for a source of the same thickness electroplated directly on a 2.25-mg/cm^2 backing. Within the statistical uncertainty, no systematic variation in the asymmetry or in the scattered intensity appears between the data obtained with the directly plated sources and those taken with supplementary backings.

The variation of the symmetry with backing thickness is shown in Fig. 6. Again, weighted least-squares fits using quadratic functions were attempted in addition to the linear ones presented here, and behavior similar to that found for the variation of asymmetry with scatterer thickness was observed. No consistent (in sign) quadratic effect was found and the effect of the quadratic fits on the extrapolations were smaller than the errors in the linear extrapolations. The percentage of backscattered electrons was estimated by fitting a quadratic function to the plot of counting rate versus backing thickness. Since the electron intensity increases almost linearly with backing thickness for backing thickness less than 1 mg/cm^2, the coefficient of the leading term gives the percent backscattered intensity in this range. Figures 7(a) and 7(b) summarize these results. The data indicate that the percent depolarization is considerably less than the percent backscattering for the lower energies studied.

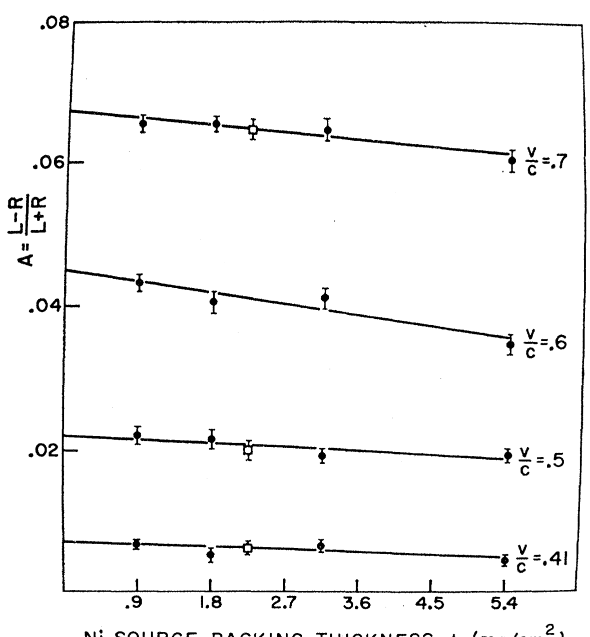

FIG. 6. Measured asymmetry obtained with the 302-μg/cm^2 scatterer plotted against source-backing thickness. The data represented by the open squares were obtained with a source plated directly on a Ni backing of 2.5-mg/cm^2 thickness. The other points were determined by varying the thickness of additional Ni foils placed 0.001 in. behind the 0.9-mg/cm^2 Ni backing. Weighted linear least-squares fits are shown.

4. Scattering within Source

Because of the availability of high-specific-activity Co^{60}, it was possible to obtain the asymmetry dependences discussed above with a source surface density of only 345 ± 17 μg/cm^2. A small contribution to the depolarization was therefore anticipated from internal source scattering. Attempts to calculate this effect have been made by Mühlschlegel and Koppe,[21] by Wegener,[8] and by Gluckstern.[22] The calculations lead to depolarization predictions between 0.3 and 9% over the range of energies investigated. More recent work by Scott[23] indicates that these calculations overestimate the depolarization.

An attempt was made to detect a source-thickness effect by repeating the asymmetry measurements with the 302-μg/cm^2 scatterer using a 170 ± 8-μg/cm^2 source. The depolarization is expected to increase with decreasing energy, but the data show no systematic increase in asymmetry using the thinner source, nor do they indicate any tendency to increase relative to the 345-μg/cm^2 source with decreasing energy. The measurements indicate that the maximum depolarization due to source scattering was less than 3% at the lowest energy.

5. Inelastic Scattering and Surface Contributions

The effect of inelastic scattering of atomic electrons on the Mott asymmetry has been calculated in a modified first Born approximation by Felsner and Rose.[24] They conclude that for gold the inelastic scattering asymmetry is approximately one-half that for Mott scattering and opposite in sign. However, since the cross section for inelastic scattering is less than 1% of the Mott scattering cross section, a correction of at most 0.5% is necessary. The average energy loss in these processes is less than 1 keV for foil thicknesses

[21] B. Mühlschlegel and H. Koppe, Z. Physik **150**, 474 (1958).
[22] R. L. Gluckstern (private communication).
[23] W. T. Scott, Rev. Mod. Phys. **35**, 231 (1963).
[24] G. Felsner and M. E. Rose, Nuovo Cimento **20**, 33 (1961).

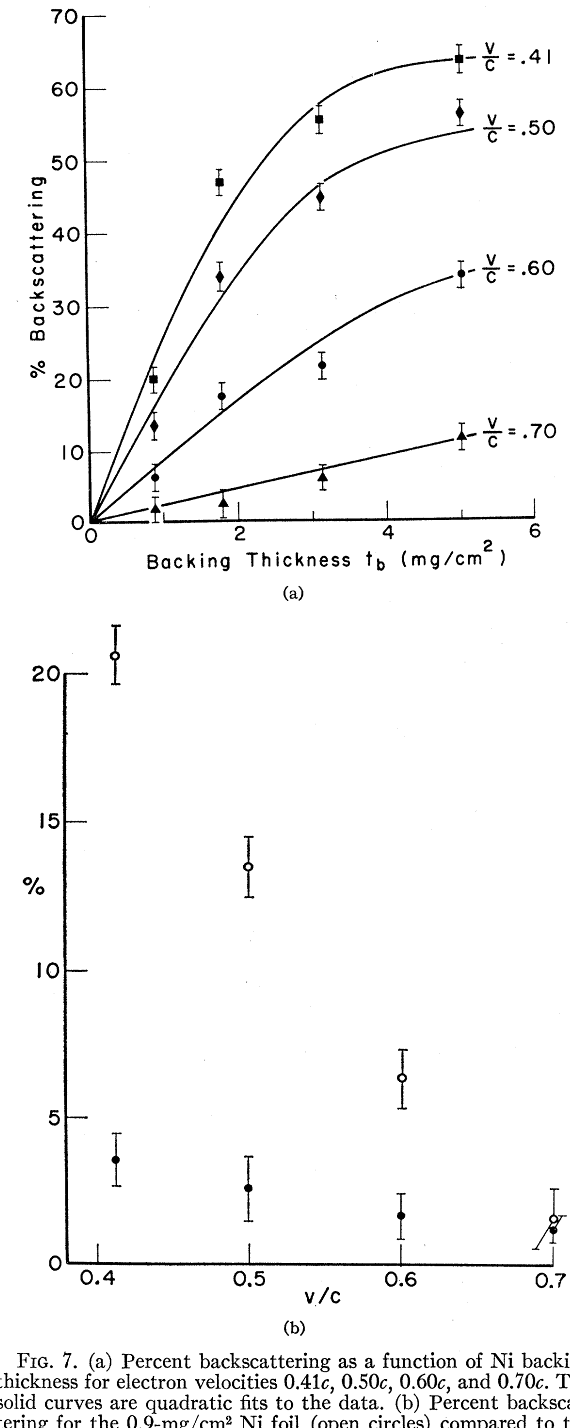

FIG. 7. (a) Percent backscattering as a function of Ni backing thickness for electron velocities 0.41c, 0.50c, 0.60c, and 0.70c. The solid curves are quadratic fits to the data. (b) Percent backscattering for the 0.9-mg/cm² Ni foil (open circles) compared to the percent depolarization (closed circles) as a function of v/c of the electrons.

used in this experiment, so that inelastically scattered electrons are not readily distinguished from those elastically scattered.

The simultaneous accumulation of full width at half-maximum (FWHM) and integral data by means of single-channel and integral discriminator outputs allows by comparison an estimate of the influence of electrons detected with energies outside the main scattered peaks. The presence of these electrons is mainly due to scattering down the deflector plates, scattering from chamber walls, and outscattering from the detector surface. The appearance of spectra taken with a detector at the scatterer position was almost identical to the scattered spectra, indicating a small contribution to the low-energy tail by electrons scattered within the scattering chamber. This was confirmed by the small increase in the tail of the scattered spectra when the collimators were removed from the detectors. A 30% increase resulted when the Teflon tubing, which was used to baffle the primary beam, was removed.

The asymmetries obtained from the entire scattered spectra (integral) were consistently 1 to 5% lower than those derived from the FWHM data. The magnitude of the difference, coupled with the large ratio of Mott-scattered electrons to those resulting from other events within the full width at half-maximum, indicates that for these data such effects contribute less than 1% reduction in the asymmetry for the FWHM data.

III. RESULTS AND DISCUSSION

The helicity of the β particles is computed from the linearly extrapolated value of the inverse of the symmetry as a function of scatterer thickness with corrections for backscattering and source scattering. From Eq. (6) it is seen that the transverse polarization is given by

$$P_T = -\frac{BS}{(1/A)_{t=0}S(\theta)}, \tag{7}$$

where B is the backscattering correction, S the source-thickness correction, and $(1/A)_{t=0}$ the value of the inverse of the asymmetry extrapolated to zero scatterer thickness.

The extensive calculations of $S(\theta)$ and $d\sigma/d\Omega(\theta)$ from potentials chosen to include the screening of the nuclear charge by atomic electrons by Lin[15] and by Holzwarth and Meister[16] are not in good agreement. Discrepancies of several percent exist at large scattering angles. The work of Holzwarth and Meister has been criticized by Bühring,[17] whose more recent calculations agree with Lin's. The recent experiment of Kessler and Weichert[25] also supports Lin's results. Lin's tabulations[15,26] for $S(\theta)$ are used here, averaged to take into account the distribution of scattering angles in the experimental situation:

$$\bar{S}(\theta) = \int\int S(\theta)\frac{d\sigma}{d\Omega}(\theta)d\Omega \Big/ \int\int \frac{d\sigma}{d\Omega}(\theta)d\Omega. \tag{8}$$

To perform this integration a Taylor-series approxi-

[25] J. Kessler and N. Weichert, Z. Physik **212**, 48 (1968).
[26] S. R. Lin (private communication).

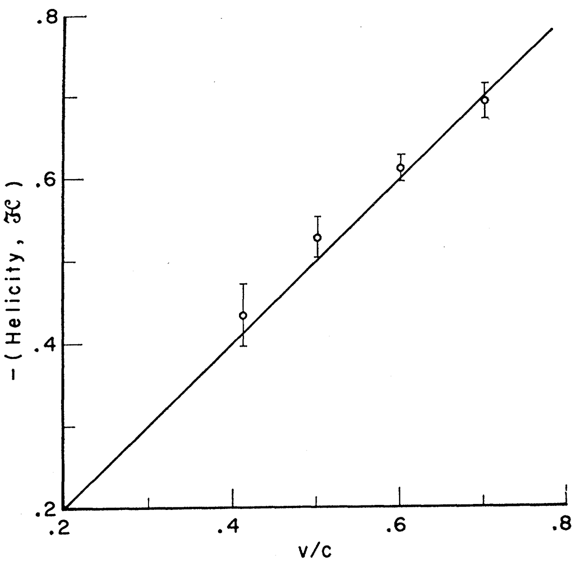

FIG. 8. Helicity plotted against v/c. The straight line represents the prediction of the $V-\lambda A$ theory with two-component neutrinos. The results were obtained from our data using Lin's calculation of $S(\theta)$ and $d\sigma/d\Omega$ (θ) (see Refs. 15 and 26). The measured helicities for $v/c=0.70$, 0.60, 0.50, and 0.41 are, respectively, $-(0.692\pm0.021)$, $-(0.611\pm0.017)$, $-(0.528\pm0.024)$, and $-(0.435\pm0.038)$.

mation was developed by Lin and Gluckstern.[26] Monte Carlo calculations yielded results within 1% of Lin's $\bar{S}(\theta)$. Table II gives $S(\theta)$ for screened nuclei as calculated by Lin,[15,26] the corrections due to the finite detector and scatterer size, and the values of $\bar{S}(\theta)$.

The function $S(\theta)$ was further averaged over the finite energy spread of the electron beam. Because of the near constancy of the product of asymmetry and differential cross section and relatively small energy spread in the beam, the values of $S(\theta)$ listed in Table II are altered by less than 0.2%.

Equation (7) gives the transverse polarization of the electron beam. The relative precession of the momentum and polarization vectors in the electrostatic analyzer differs from the angle of rotation of the momentum

TABLE II. Mott asymmetry function $S(\theta)$, corrections for finite angular spread, and the average $\bar{S}(\theta)$ of $S(\theta)$ over the distribution of scattering angles in the experimental situation.

v/c	$S(\theta)$	Geometric correction (%)	$\bar{S}(\theta)$
0.7	−0.1303	4.06	−0.1250
0.6	−0.1243	5.47	−0.1175
0.5	−0.10155	6.59	−0.09486
0.41	−0.06155	9.07	−0.05606

vector because of the magnetic field experienced by the electrons as a result of their motion in the electric field. For a rotation of the momentum vector by an angle ψ, the actual relative precession angle differs from $\frac{1}{2}\pi$ by[27]

$$\psi'=\tfrac{1}{2}\pi-\psi[\tfrac{1}{2}g(1-\beta^2)^{1/2}-(\tfrac{1}{2}g-1)(1-\beta^2)^{-1/2}],$$

where g is the electron gyromagnetic ratio including electrodynamic corrections, so that

$$P_T=\mathcal{H}\sin(\tfrac{1}{2}\pi-\psi'). \tag{9}$$

For $\psi=\frac{1}{2}\pi$, ψ' varies from 8° to nearly 25° in the range $v/c=0.4$ to 0.7.

The helicities $\mathcal{H}$ obtained from Eqs. (7)–(9) are plotted against v/c in Fig. 8. The error limits shown include all the uncertainties in the systematic corrections discussed above. The weighted mean of the four helicity measurements is $-\mathcal{H}/(v/c)=1.014\pm0.018$. The error quoted is 1 standard deviation, which includes all known experimental sources of error. Errors in the calculated quantities such as $S(\theta)$ are not included in this result.

The low values for the helicity obtained by other workers[8–10] at the lower energies are not observed here. In particular, the large source-scattering depolarization effects reported by Eckardt, Ladage, and Moellendorff[9] are not reproduced in these measurements.

For an allowed Gamow-Teller transition, assuming time-reversal invariance but not including contributions from higher-order transitions, finite-nuclear-size effects, and screening by atomic electrons, the electron helicity is given by[28]

$$\mathcal{H}=\frac{2(v/c)[C_TC_T'-C_AC_A']}{|C_T|^2+|C_T'|^2+|C_A|^2+|C_A'|^2+2(m/E)\gamma(C_TC_A+C_T'C_A')}, \tag{10}$$

where

$$\gamma=[1-(\alpha Z)^2]^{1/2}.$$

For the $V-\lambda A$ interaction, the helicity becomes

$$\mathcal{H}=-2(v/c)\frac{C_A'/C_A}{1+(C_A'/C_A)^2}. \tag{11}$$

Alternatively, for two-component neutrinos (left handed), but allowing tensor interaction admixture, the helicity of the β particles becomes

$$\mathcal{H}=-(v/c)\left[\frac{1-(C_T/C_A)^2}{1+(C_T/C_A)^2+2(m/E)\gamma C_T/C_A}\right]. \tag{12}$$

The way in which this series of measurements of the

[27] V. Bargman, L. Michel, and V. L. Telegdi, Phys. Rev. Letters 2, 435 (1959).
[28] J. D. Jackson, S. B. Treiman, and H. W. Wyld, Jr., Phys. Rev. 106, 517 (1957).

electron helicity limits the ratios C_A'/C_A and C_T/C_A, each under the appropriate assumption regarding the other, is apparent from Eqs. (11) and (12). Sequentially assigning the deviation from $\mathcal{H}=-v/c$ permitted by an experimental uncertainty of 1 standard deviation to a departure from the two-component neutrino theory and then to an admixture of the tensor interaction limits the ratio C_A'/C_A to values between 0.90 and 1.11 and the ratio $C_T/C_A<0.0029$.

Combining these results with the results of other measurements at higher energies,[6] the v/c dependence of the helicity required by the two-component neutrino hypothesis has now been verified from $v/c=0.4$ to 0.9 for allowed Gamow-Teller transitions. The present level of accuracy precludes the observation of small corrections due to higher-order transitions, finite nuclear size, and screening by atomic electrons.[29] Of these, the latter is expected to produce the largest effect: a reduction of the polarization by a fraction of 1% at the higher momenta and by 2% at $v/c=0.41$. It would be difficult to extend these measurements to lower energies, or sufficiently improve the accuracy with the present techniques so that a significant improvement in the determination of the coupling constant could be obtained. We point out again, however, that the helicities for the Fermi transitions are presently only poorly determined.

[29] W. Bühring, Nucl. Phys. 40, (1963); 61, 110 (1965).

ACKNOWLEDGMENTS

We wish to thank Professor S. R. Lin and Professor R. L. Gluckstern for the calculations of the asymmetry function, cross sections, and multiple scattering effects as well as many helpful discussions. We gratefully acknowledge the assistance of Professor K. S. R. Sastry and Richard Treffers. Irwin Gruverman of New England Nuclear Corporation prepared the sources. We wish to thank Professor V. W. Hughes for his continued interest and support.

PHYSICAL REVIEW D VOLUME 2, NUMBER 1 1 JULY 1970

Photoproduction of Electron-Positron Pairs at 2.3 and 5.6 GeV†*

J. TENENBAUM,‡ A. M. EISNER,§ G. J. FELDMAN,§ W. LOCKERETZ, F. M. PIPKIN, AND J. K. RANDOLPH‖
Cyclotron Laboratory, Harvard University, Cambridge, Massachusetts 02138
(Received 27 February 1970)

We have measured the photoproduction of electron-positron pairs from carbon using an improved version of the Harvard pair spectrometer. The bending magnet and two half-quadrupole magnets were retained. For each half-quadrupole, a tungsten collimator was added at the entrance, a portion of the lead obstacle was removed, and a defining counter was added at the midpoint. Faster counting electronics and an on-line computer were employed. Pairs were detected in an invariant-mass range of 97–445 MeV. The results are in agreement with the predictions of quantum electrodynamics and may be parametrized as $R=(1.09\pm0.07)\times[1+(31.6_{-41.2}^{+31.2})\times10^{-8}Q_M^2]$. Here R is the ratio of experiment to theory, and Q_M^2 is the electron-pair mass squared (GeV$^2/c^4$). The errors include both statistical and systematic effects. In the course of this work, we have also derived an accurate approximation for the electron-pair cross section.

I. INTRODUCTION

THE modern formulation of quantum electrodynamics (QED) resulted from the work of Feynman, Schwinger, and Tomonaga. The Lamb shift in hydrogen and the radiative correction to the gryomagnetic ratio of the electron gave the first confirmation of the theory. These radiative effects are sensitive to the high-energy behavior of the virtual particles in the higher-order Feynman diagrams. Since the contribution of the higher-order diagrams is small, the measurements must be made to high precision in order to check the theory. The current situation for low-energy tests of QED has been reviewed by Brodsky.[1] At present the experimental values for the Lamb shift and the gyromagnetic ratio of the electron do not agree with the theoretical values. The most sensitive test, the gyromagnetic ratio of the muon, gives agreement between experiment and theory.

During the past ten years, high-energy experiments have been used to give a different kind of test of QED. The precision is less than that of atomic physics experiments, but the experiments are more directly sensitive to the high-energy behavior. Drell[2] suggested that a breakdown of QED might occur in three different

† Work supported by the U. S. Atomic Energy Commission under Contract No. AT(30-1)2752.

* Paper based in part on a thesis submitted by one of the authors (JT) to Harvard University in partial fulfillment of the requirements for the Doctor of Philosophy in Physics.

‡ Present address: Stanford Linear Accelerator Center, Stanford, Calif.

§ National Science Foundation Graduate Fellow.

‖ Present address: Randall Laboratory of Physics, University of Michigan, Ann Arbor, Mich.

[1] S. J. Brodsky, in *International Symposium on Electron and Photon Interactions at High Energies, Liverpool, England, 1969*, edited by D. W. Broben (Daresbury Nuclear Physics Laboratory, Daresbury, Lancashire, England, 1970), p. 3.

[2] S. D. Drell, Ann. Phys. (N. Y.) 4, 75 (1958).